DNA tile self-assembly guided by base excision repair enzymes

Nada Farag,[a] Gianfranco Ercolani,[a] Erica Del Grosso,[a] Francesco Ricci*[a]

[a] N. Farag, G. Ercolani, E. Del Grosso, F. Ricci
Department of Chemical Sciences and Technologies
University of Rome Tor Vergata
Via della Ricerca Scientifica, 00133 Rome, Italy
E-mail: francesco.ricci@uniroma2.it

Supporting information for this article is given via a link at the end of the document

Abstract: We demonstrate here the use of DNA repair enzymes to control the assembly of DNA-based structures. To do so, we employed Uracil-DNA Glycosylase (UDG) and Formamidopyrimidine DNA Glycosylase (Fpg), two enzymes involved in the base excision repair pathway. We designed two responsive nucleic acid modules containing mutated bases (deoxyuridine or 8-oxo-7,8-dihydroguanine recognized by UDG and Fpg, respectively) that, upon the enzyme repair activity, release a nucleic acid strand that induces the self-assembly of DNA tiles into tubular structures. The approach is programmable, specific and orthogonal and the two responsive modules can be used in the same solution without crosstalk. This allows to assemble structures formed by two different tiles in which tiles distribution can be accurately predicted as a function of the relative activity of each enzyme. Finally, we show that BER-enzymes inhibitors can also be used to control DNA-tile assembly in a specific and concentration-dependent manner.

Introduction

DNA damage caused by various endogenous and exogenous agents may induce mutations leading to genomic instability and carcinogenesis.[1,2] DNA repair enzymes represent an important class of enzymes that are deputed to maintain genomic integrity by recognizing and correcting these DNA anomalies through different mechanisms.[3,4] One of the most important repair mechanisms is the base excision repair (BER) pathway which involves more than 30 enzymes that through concerted action can recognize and preserve the integrity of DNA.[5,6] BER pathway proceeds through the recognition and then removal of the damaged bases by damage-specific DNA glycosylases such as Uracil DNA Glycosylase and Oxoguanine Glycosylase enzymes.[7–9] These enzymes have thus gained growing importance as biomarkers and potential therapeutic targets in many diseases.[10,11] Developing new biotechnology systems that are controlled by these enzymes could lead to new tools with possible sensing and drug-delivery applications.[12–14]

In the last two decades, DNA nanotechnology has emerged as a promising approach to create biomolecular devices made of synthetic nucleic acids that can find applications in both sensing and drug delivery.[15–17] Synthetic nucleic acids can be for example used as building block materials to assemble programmable DNA-based structures[18–20] that can be decorated with Ångstrom-like precision with a variety of different chemical and biological species. These structures can be programmed to respond to different inputs leading to their assembly/disassembly or spatial reconfiguration that can be ultimately associated with the emission of a measurable signal or the release of therapeutic cargo.[21–25] DNA-structures responsive to a variety of chemical and environmental cues including DNA sequences,[26,27] small molecules,[28,29] antibodies,[22,30] pH[31,32] ,temperature,[33] and light[34–36] have been described to date. However, the use of DNA repair enzymes as molecular cues to control the assembly of similar DNA-based structures have not yet been demonstrated, a gap that appears surprising if one considers the relevance and diversity of these enzymes.

Motivated by the above considerations, here we propose to control the self-assembly process of DNA-based structures in a predictable and orthogonal way using BER enzymes. To demonstrate this, we employed double-crossover DNA tiles (DAE-E) formed through the hybridization of five different synthetic DNA strands and displaying four 5-nt sticky ends (red portions, Figure 1a) that allow their spontaneous self-assembly into micron-scale hollow tubular polymeric structures.[37–39] Previous reports have shown that the ability of these tiles to self-assemble can be reversibly inhibited by a DNA strand (invader or inhibitor) that blocks one of the four sticky ends and can subsequently be activated by another DNA strand (anti-invader or activator) that displaces the inhibitor from the tile with a strand displacement reaction[31,39] (Figure 1a). To control DNA-tile assembly with BER enzymes, we have rationally designed ds-DNA responsive modules containing different DNA mutated bases targeting different BER enzymes (Figure 1b). The activity of a specific BER enzyme on the mutated bases of the responsive module creates abasic sites (or nick) that destabilize the duplex inducing the consequent release of a DNA activator strand. This can in turn activate the DNA tiles and initiate the spontaneous self-assembly of tubular structures (Figure 1b).

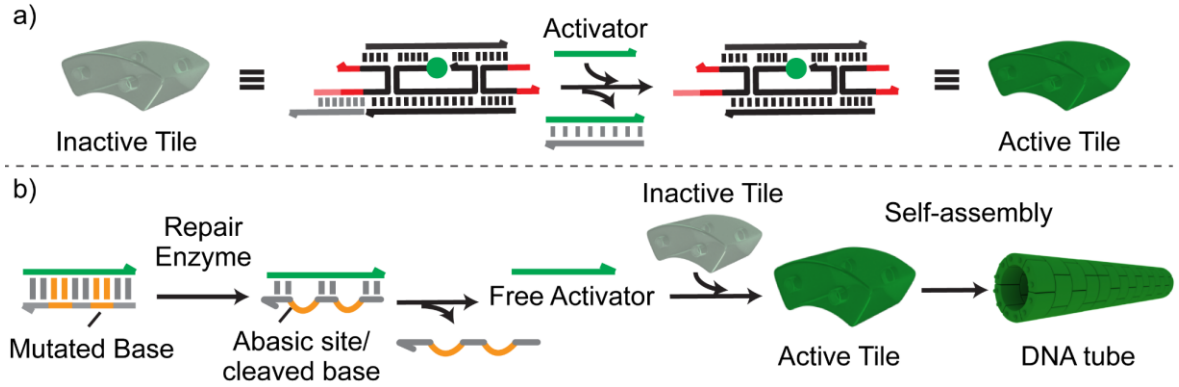

Figure 1. Self-assembly of DNA tiles guided by base excision repair (BER) enzymes. a) Scheme of tile activation. An inactive DNA tile in which one of the four sticky ends (red) is blocked by an inhibitor strand (grey) can be activated by an activator strand (green) that displaces, through a toehold mediated strand displacement reaction, the inhibitor. b) Scheme of tile self-assembly guided by a BER enzyme. Repair enzyme-responsive duplex module formed by the activator strand and a complementary strand containing mutated bases. A site-specific BER enzyme specifically targets the mutated base leading to the formation of abasic sites (or nick, not shown) that, by destabilizing the duplex, leads to the release of the activator strand. Once released, the activator strand induces the activation of the DNA tiles that self-assemble into tubular polymeric structures. DNA tiles are depicted here as LEGO-like brick models where knobs and holes represent the four sticky ends.

Results and Discussion

As the first test-bed for our strategy, we employed Uracil-DNA Glycosylase (UDG), a base-excision repair enzyme that hydrolyzes deoxyuridine mutations from ssDNA or dsDNA strands leading to the formation of abasic sites.[5,40] We designed a UDG-responsive module formed by a tile-activator strand (green) and a complementary strand (black) containing 4 deoxyuridine lesions. The presence of UDG induces the formation of abasic sites at the deoxyuridine sites destabilizing the responsive duplex and leading to the release of the activator strand (Figure 2a) and downstream activation of the DNA tiles.

We first demonstrated successful UDG-induced activator release with a fluorescent-labeled UDG-responsive module using fluorescence time-course experiments (Figure 2a-b) and native-PAGE electrophoresis (Figure S1). As expected, the rate of activator release follows a UDG concentration-dependent behavior in a UDG concentration range between 0.1 and 20 U/ml (Figure 2b, S1). We then demonstrated that the released activator can efficiently activate DNA tiles. To do this without the complications of the self-assembly process, we initially employed control tiles lacking the sticky ends thus unable to self-assemble into tubular structures (Figure 2c). The inactive tiles were labeled with a fluorescence optical pair (Cy5/Cy3) that is separated by the interaction with the activator strand so an increase in fluorescence signal indicates tiles activation (Figure S2). Also, in this case, the kinetic of this process follows a UDG concentration-dependent behavior (Figure S3). More specifically, the half-life of the tile activation process ($t_{½\_Act}$, time at which 50% of the DNA tiles are activated) decreases from 230 ± 5 min to 1.9 ± 0.2 min) by increasing the UDG concentration from 0.1 to 20 U/ml, respectively (Figure 2d).

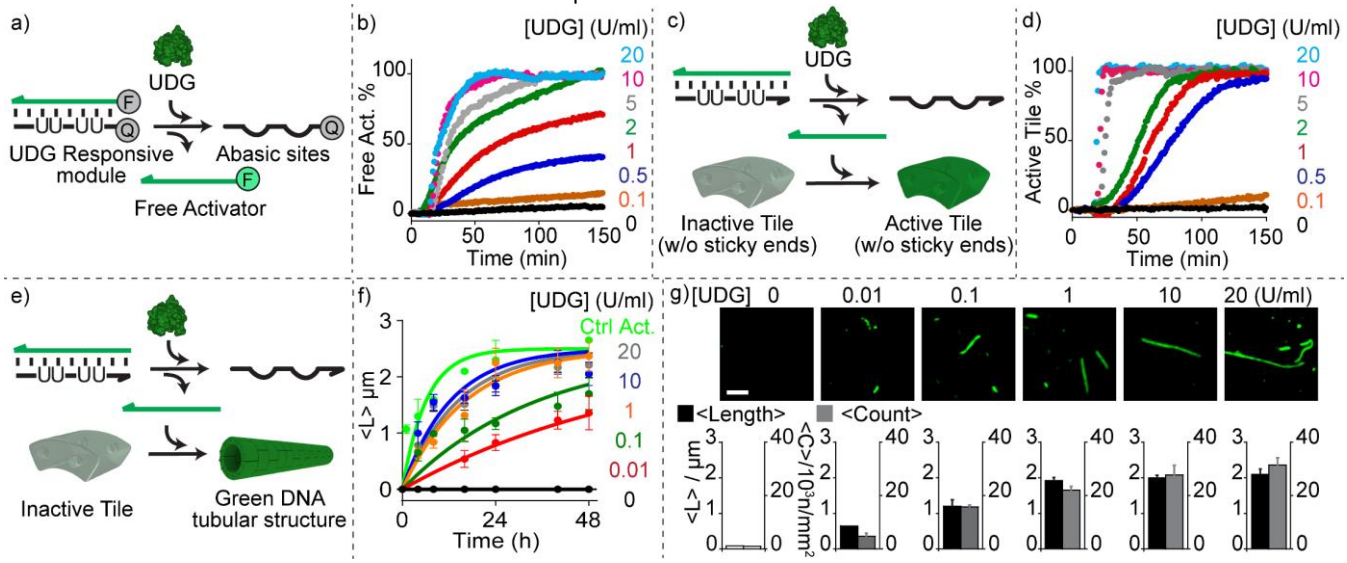

Figure 2. DNA tile self-assembly guided by Uracil DNA Glycosylase (UDG). a) Scheme of UDG-responsive module labeled with a Cy5/BHQ2 pair. Activator release is followed by a signal increase after UDG addition. b) Time-course fluorescent experiments showing activator release (as %) at different UDG concentrations. c) Scheme of UDG-guided tile activation using tiles lacking sticky ends. d) Half-time of tile activation vs. UDG concentrations. e) Scheme of UDG-guided DNA tile self-assembly. f) DNA structures assembly kinetics (average length, <L>, vs time at different UDG concentrations. g) Fluorescence microscope images of DNA structures at different UDG enzyme concentrations. The bar plots below each image represent the average length (<L>, µm) and count (<C>, number of structures/mm^2) of the formed DNA structures. All experiments were performed at 30 °C in 20 mM Tris-HCl, 10 mM $MgCl_2$, 1 mM EDTA, 0.1 mg/ml BSA, pH 8.0 buffer solution containing the UDG-responsive module (0.7 µM), inactive tiles (with and without sticky ends) (0.35 µM) and the indicated UDG concentration. Panel g shows the structures after 24 hours of reaction. The error bars reflect the standard deviations of three separate measurements. Images scale bar: 2.5µm.

To demonstrate that UDG can be used to control the assembly of DNA-based structures, we have then tested the above described UDG-responsive module with inactive tiles containing sticky-ends (Figure 2e). To follow structures assembly through fluorescence microscopy, the tiles were internally labeled with a fluorescent dye (Q670). While in the absence of UDG, no structures were observed even after 48 h of incubation (Figure 2f), UDG concentration-dependent assembly kinetic was observed by increasing the UDG concentration from 0.01 to 20 U/ml (Figures 2f-g, S4). The average length (<L>, μm) of the DNA nanostructures after 24 hours of enzymatic reaction increased from 0.6 ± 0.1 μm to 2.1 ± 0.2 μm by increasing UDG concentrations from 0.01 U/ml to 20 U/ml respectively. A similar trend was also observed for the total number of structures observed (<C>, number of structures/mm^2) (Figures 2g, S5).

To further demonstrate the versatility of our approach, we then moved to Formamidopyrimidine DNA Glycosylase (Fpg), a bifunctional enzyme that detects and releases 8-oxo-7,8-dihydroguanine (G^{oxo}) generating a 1-nucleotide DNA gap in the DNA strand.[41,42] We have rationally designed an Fpg-responsive duplex module in which one of the two strands contains an internal G^{oxo} base that separates an 11-nt random sequence (black domain, Figure 3a) from the activator sequence (red domain, Figure 3a). Upon addition of Fpg, the G^{oxo} mutated base is removed leading to the destabilization of the responsive module and subsequent release of the activator (Figure 3a). We first demonstrated Fpg-dependent activator release using native-PAGE electrophoresis (Figure 3b). We also followed DNA tiles activation after the Fpg-induced activator release using control tiles lacking the sticky ends and observed an Fpg concentration-dependent behavior (Figures 3c-d, S6). The half-life of tile activation ($t_{½\_Act}$) decreases from 40.0 ± 0.8 h to 1.0 ± 0.2 h by increasing Fpg concentration from 1 to 100 U/ml (Figure S7). To investigate Fpg-induced assembly of DNA-based structures through fluorescence microscopy, we have tested the Fpg-responsive module with inactive tiles containing sticky-ends and labeled with a fluorophore (Q570) (Figure 3e). In the absence of Fpg, no structures were observed even after 48 h of incubation (Figure 3f). Fpg concentration-dependent assembly kinetic was observed at varying Fpg concentrations (Figures 3f, g, S8). The average length (<L>, μm) of the DNA structures after 24 hours of enzymatic reaction increased from 1.3 ± 0.2 μm to 3.6 ± 0.3 μm by increasing Fpg concentrations from 5 U/ml to 100 U/ml respectively. A similar trend was also observed for the total number of structures observed (<C>, number of structures/mm^2). (Figures 3g, S9).

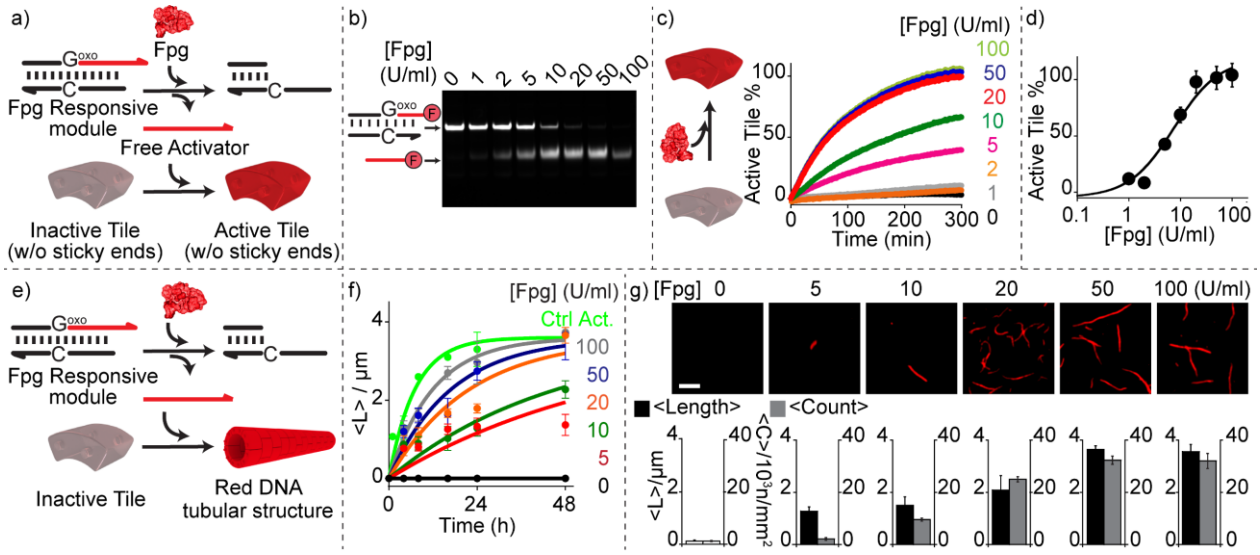

Figure 3. DNA tile self-assembly guided by Formamidopyrimidine DNA Glycosylase (Fpg). a) Fpg-guided activator release studied using tiles lacking sticky ends. b) Native-PAGE of Fpg-guided activator release at varying Fpg concentrations. c) Kinetic traces of DNA tile activation (%) at different Fpg concentrations. d) Active DNA tiles (%) (end-point from panel c) vs. Fpg concentrations. e) Fpg-guided DNA structure self-assembly. f) DNA structures assembly kinetics at different Fpg concentrations. g) Fluorescence microscope images obtained at different Fpg enzyme concentrations. The bar plots below each image represent the average length (<L>, μm) and count (<C>, number of structures/mm2) of the formed DNA structures. All experiments were performed at 30 °C in 20 mM Tris-HCl, 10 mM MgCl2, 1 mM EDTA, 0.1 mg/ml BSA, pH 8.0 buffer solution containing the Fpg-responsive module (0.7 μM), inactive tiles (with and without sticky ends) (0.35 μM) and the indicated Fpg concentrations. For the native-PAGE experiment, the enzymatic reaction time was 2 h. Panel g shows the structures after 24 hours of reaction. The error bars reflect the standard deviations of three separate measurements. Images scale bar: 2.5μm.

The responsive modules we describe here are orthogonal and can work in the same solution without cross-talk. To demonstrate this, we employed in the same solution the two responsive modules described above and coupled them with two different DNA tiles that share the same sticky ends and can thus co-assemble in a single polymer structure containing both tiles (DNA co-polymer). Each tile is activated by a specific activator strand released by a specific repair enzyme (Figure 4a). The two tiles are also labeled with two different fluorophores (Q670 and Q570) so they can be easily distinguished by fluorescence microscopy. By varying the concentrations of the two repair enzymes we can control the distribution of the tiles in the assembled DNA tubular co-polymer. By doing this, we can achieve green (Figure 4b, left) or red (Figure 4b, right) homo-polymers (thus formed by a single tile) when only one of the two enzymes is present. Conversely, when the activity of both enzymes becomes comparable, we achieve co-polymer structures with a statistical distribution of green and red tiles (Figure 4b, center and Figure S10). The distribution of the two active tiles in the assembled DNA polymers is conveniently

measured by the mole fraction of the two active tiles (χ_G and χ_R). For example, homo green structures are formed when only green active tiles are present in solution (i.e., $\chi_G = 1$), while an equal distribution of green and red tiles is observed when $\chi_G = \chi_R = 0.5$. The distribution of the enzyme-guided tiles assembly depends on the rate at which the inactive green and red tiles are activated. Thus, taking into consideration the previously observed assembly rate of green and red tiles controlled by UDG and Fpg (Figures 2f, 3f), we can predict by a kinetic scheme (Scheme S1-S3) the mole fraction χ_G for a series of experiments with variable concentrations of the two enzymes. It was gratifying to observe a very good agreement between the experimental molar fraction χ_G and the predicted ones (R^2=0.99) (Figure 4c, S10, Tables S1-S2).

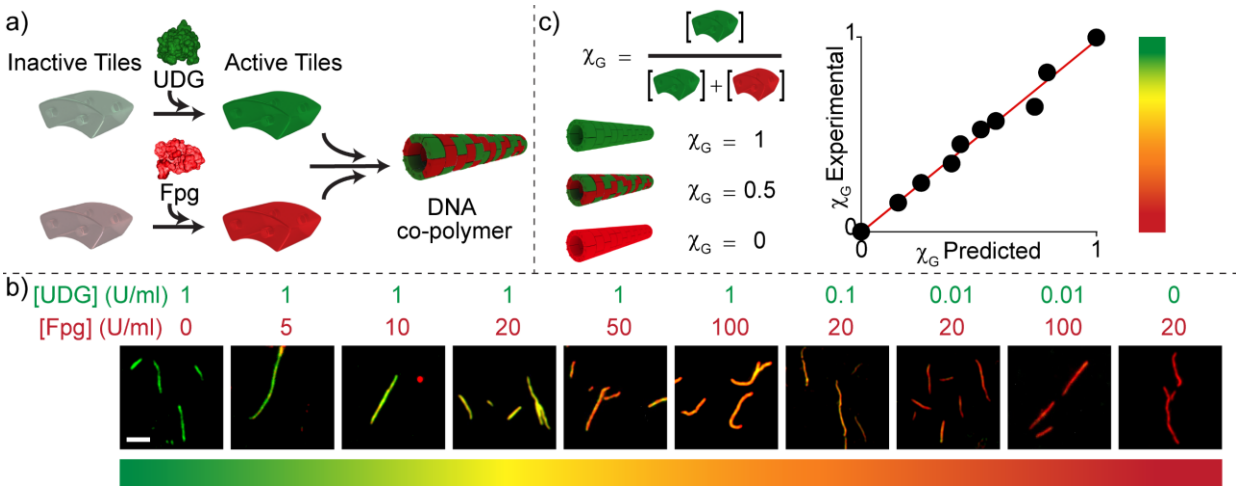

Figure 4. Controlling tile distribution in DNA co-polymers with two base excision repair enzymes. a) Scheme of random DNA co-polymers assembly guided by UDG and Fpg enzyme. b) Fluorescence microscope images of structures obtained at different UDG and Fpg concentrations. c) Plot of experimental vs. predicted mole fraction of active green tiles (χ_G) in DNA structures. The straight line with slope 1 and intercept 0 would represent a perfect agreement between predicted and experimental χ_G values. Scale color in the y-axis correlates with the observed color of the assembled structures (panel b). The experiments were performed at 30 °C for 24 h in 20 mM Tris-HCl, 10 mM $MgCl_2$, 1 mM EDTA, 0.1 mg/ml BSA, pH 8.0 buffer solution containing an equimolar concentration of UDG, Fpg-responsive modules (0.7 μM), equimolar concentration of inactive green/ red tiles (0.35 μM) and different concentrations of UDG and Fpg. Scale bar: 2.5μm

We further tested the possibility to reversibly control assembly/disassembly of DNA tiles using both enzymes in the same solution. To do this, we employed the above-characterized Fpg-responsive module inducing the activation of DNA tiles (Figure 3). We also engineered and experimentally characterized a new UDG-responsive module in which the UDG repair activity leads to the release of an invader strand (i.e. a strand that, by binding to one of the sticky ends, induces the disassembly of the DNA tubular structures) [39] (Fig. 5a, S11). We mixed the two responsive modules in the same solution together with inactive tiles. The addition of Fpg leads, as expected, to formation of tubular structures (Fig. 5b). The following addition of UDG leads to the release of the invader strand and complete disassembly of the formed structures (Fig. 5b).

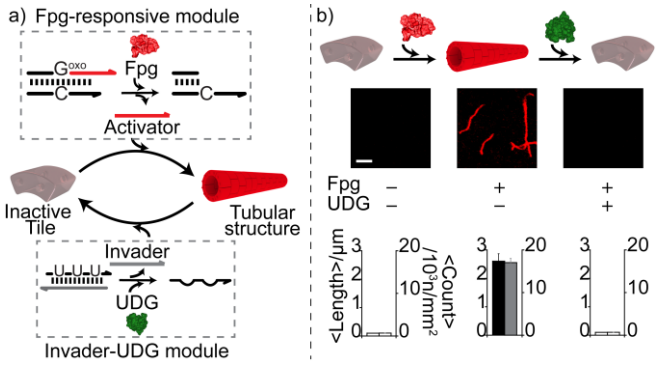

Figure 5. Reversible assembly/disassembly of DNA tiles guided by BER enzymes. a) Scheme of DNA tiles assembly by Fpg-guided activator release and disassembly by UDG-guided invader release. b) Fluorescence microscope images for assembled/disassembled DNA tiles obtained after addition of Fpg and UDG. The bar plots below each image represent the average length (<L>, μm) and count (<C>, number of structures/mm^2) of the formed DNA structures. The experiments were performed at 30 °C in 20 mM Tris-HCl, 10 mM $MgCl_2$, 1 mM EDTA, 0.1 mg/ml BSA, pH 8.0 buffer solution containing Fpg-responsive module (0.7 μM), invader-UDG-responsive module (0.35μM), inactive tiles (0.35μM). Fpg (20U/ml) was added, and images taken after 24 h. UDG (10U/ml) was then added, and new images were taken after 2 h. Scale bar: 2.5μm.

Prompted by the above results, we then demonstrated the possibility to control DNA tiles activation using base excision repair inhibitors. To do so, we followed DNA tiles assembly guided by UDG or Fpg in the presence of specific inhibitors of these two enzymes. Firstly, we tested Uracil Glycosylase Inhibitor (UGI), a small protein that inhibits UDG enzymatic activity by forming a stable UDG-UGI protein complex.[43,44] We observe a UGI concentration-dependent decrease in the average length (<L>, μm) of the assembled DNA tubular structures at increasing UGI concentrations. No visible structures were observed at UGI concentrations above 10 U/ml (Figure 6a, S12). To inhibit the Fpg-guided tile assembly, we used 2-thioxanthine (2TX) as an inhibitor for Fpg enzymatic activity.[45,46] Also here, we observed a 2TX concentration-dependent decrease in the average length (<L>, μm) of the assembled DNA tubular structures at increasing 2TX concentrations. No visible structures were observed at 2TX concentrations above 10 mM (Figure 6b, S13). Since each inhibitor selectively inhibits its target enzyme, we then studied the possibility to control the activation of two different tiles in the same solution using two different BER inhibitors. Also in this case, we employed two tiles sharing the same sticky ends but activated by two different strands. We can selectively control the activation of each tile (Figure 6c). For example, in the absence of the two inhibitors, both tiles are activated and assembled into DNA co-polymers with a statistical distribution of both tiles (Figure 6c, S14).

By adding only one inhibitor we can guide the formation of green or red homo-polymers. We can also control the statistical distribution of each tile in the assembled DNA co-polymer by varying the concentration of each inhibitor (Figures S15, S16).

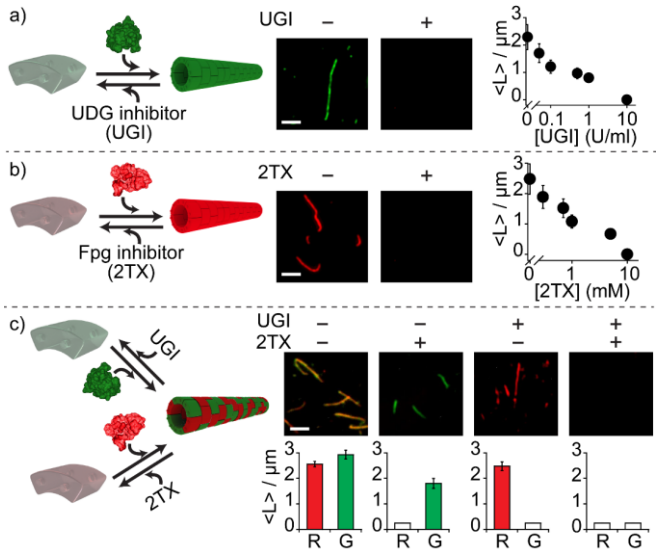

Figure 6. Controlling DNA tile self-assembly using base excision repair enzymes inhibitors. a) from left to right: scheme of self-assembly inhibition by Uracil Glycosylase Inhibitor (UGI). Microscope images in the absence and presence (10 U/ml) of UGI. Average length of assembled structures (<L>, µm) vs. UGI concentration. b) from left to right: scheme of self-assembly inhibition by 2-Thioxanthine (2TX). Microscope images in the absence and presence (10 mM) of 2TX. Average length of assembled structures (<L>, µm) vs. 2TX. c) Scheme of DNA co-polymers assembly guided by UDG and Fpg inhibitors. Microscope images and average length (<L>, µm) of the formed DNA structures with different combinations of the two inhibitors used. All the experiments were performed at 30 °C for 24 h in 20 mM Tris-HCl, 10 mM $MgCl_2$, 1 mM EDTA, 0.1 mg/ml BSA, pH 8.0 buffer solution containing equimolar concentration of UDG, Fpg-responsive modules (0.7 µM), inactive tiles (0.35 µM), UDG, Fpg (20 U/ml) in the absence or presence of UGI and 2TX. Images scale bar: 2.5µm.

Conclusion

Here we have demonstrated a strategy to control DNA tile activation and their downstream self-assembly into tubular structures using Base Excision Repair (BER) enzymes. To do this, we selected two model repair enzymes (UDG and Fpg) and rationally designed two DNA responsive modules each containing different mutated bases recognized by a specific repair enzyme. The activity of the repair enzyme on the responsive module induces the release of a DNA strand that leads to DNA tiles activation and self-assembly into tubular structures. We showed here that by varying the concentration of the enzyme, we can control the self-assembly kinetic process. Moreover, we demonstrated that the two responsive modules are orthogonal and can work in the same solution without any cross-talk. This allows us to guide the assembly of co-polymers formed by two different tiles with highly predictable distribution by simply controlling the activity of each enzyme. We have also demonstrated the reversibility of DNA tiles assembly/disassembly guided by both enzymes simultaneously. Finally, we showed that self-assembly can be further controlled using specific inhibitors of the BER enzymes employed.

While many strategies have been proposed to date to control the assembly and disassembly of DNA-based structures with different inputs (including pH, light, molecular cues, proteins, etc),[28-36] this is, to the best of our knowledge, the first demonstration of the use of BER enzymes to do so. Because of the versatility, specificity and clinical significance of BER enzymes this approach might open to possible applications in the field of sensing and drug delivery. For example, we envision that similar assembled structures can be used for imaging purposes to inform on the presence and activity of different repair enzymes in cells.[47–49] DNA structures decorated with multiple functional moieties including therapeutic agents[50,51] could also be assembled on demand in the presence of specific disease repair enzyme biomarkers. Finally, repair enzymes could be used to drive mechanical and structural changes in more complex DNA structures (including origami)[52,53] providing new biotechnology tools that can find diverse clinical applications.[47,54]

Acknowledgements

This work was supported by Associazione Italiana per la Ricerca sul Cancro, AIRC (project n. 21965) (FR), by the European Research Council, ERC (Consolidator Grant project n. 819160) (FR) and by the European Union's Horizon 2020 research and innovation program under the Marie Skłodowska-Curie grant agreement No 896962, "ENZYME-SWITCHES" (EDG).

Keywords: DNA Tiles • Self-assembly • DNA repair enzymes • DNA structures • DNA nanotechnology

[1] N. Chatterjee, G. C. Walker, *Environ. Mol. Mutagen.* **2017**, *58*, 235–263.
[2] T. Helleday, E. Petermann, C. Lundin, B. Hodgson, R. A. Sharma, *Nat. Rev. Cancer 2008 83* **2008**, *8*, 193–204.
[3] A. Ciccia, S. J. Elledge, *Mol. Cell* **2010**, *40*, 179–204.
[4] A. Sancar, L. A. Lindsey-Boltz, K. Ünsal-Kaçmaz, S. Linn, *Annu. Rev. Biochem.* **2004**, *73*, 39–85.
[5] H. E. Krokan, M. Bjørås, *Cold Spring Harb. Perspect. Biol.* **2013**, *5*, 1–22.
[6] M. L. Hegde, T. K. Hazra, S. Mitra, *Cell Res. 2008 181* **2008**, *18*, 27–47.
[7] S. D. Bruner, D. P. G. Norman, G. L. Verdine, *Nat. 2000 4036772* **2000**, *403*, 859–866.
[8] S. S. David, V. L. O'Shea, S. Kundu, *Nat. 2007 4477147* **2007**, *447*, 941–950.
[9] A. L. Jacobs, P. Schär, *Chromosoma* **2012**, *121*, 1–20.
[10] T. Visnes, A. Cázares-Körner, W. Hao, O. Wallner, G. Masuyer, O. Loseva, O. Mortusewicz, E. Wiita, A. Sarno, A. Manoilov, J. Astorga-Wells, A. S. Jemth, L. Pan, K. Sanjiv, S. Karsten, C. Gokturk, M. Grube, E. J. Homan, B. M. F. Hanna, C. B. J. Paulin, T. Pham, A. Rasti, U. W. Berglund, C. Von Nicolai, C. Benitez-Buelga, T. Koolmeister, D. Ivanic, P. Iliev, M. Scobie, H. E. Krokan, P. Baranczewski, P. Artursson, M. Altun, A. J. Jensen, C. Kalderén, X. Ba, R. A. Zubarev, P. Stenmark, I. Boldogh, T. Helleday, *Science* **2018**, *362*, 834–839.
[11] N. J. Curtin, *Nat. Rev. Cancer* **2012**, *12*, 801–817.
[12] N. Farag, R. Mattossovich, R. Merlo, Ł. Nierzwicki, G. Palermo, A. Porchetta, G. Perugino, F. Ricci, *Angew. Chemie Int. Ed.* **2021**, *60*, 7283–7289.
[13] D. L. Wilson, E. T. Kool, *J. Am. Chem. Soc.* **2019**, *141*, 19379–19388.
[14] T. Ono, S. Wang, C.-K. Koo, L. Engstrom, S. S. David, E. T. Kool, *Angew. Chemie Int. Ed.* **2012**, *51*, 1689–1692.
[15] N. C. Seeman, H. F. Sleiman, *Nat. Rev. Mater.* **2017**, *3*, 1–23.
[16] M. Lin, J. Wang, G. Zhou, J. Wang, N. Wu, J. Lu, J. Gao, X. Chen, J. Shi, X. Zuo, C. Fan, *Angew. Chemie - Int. Ed.* **2015**, *54*, 2151–2155.

[17] S. Ranallo, A. Porchetta, F. Ricci, *Anal. Chem.* **2019**, *91*, 44–59.
[18] S. Gentile, E. Del Grosso, L. J. Prins, F. Ricci, *Angew. Chemie Int. Ed.* **2021**, *60*, 12911–12917.
[19] P. Chidchob, D. Offenbartl-Stiegert, D. McCarthy, X. Luo, J. Li, S. Howorka, H. F. Sleiman, *J. Am. Chem. Soc.* **2019**, *141*, 1100–1108.
[20] H. Ramezani, H. Dietz, *Nat. Rev. Genet.* **2020**, *21*, 5–26.
[21] S. Gentile, E. Del Grosso, P. E. Pungchai, E. Franco, L. J. Prins, F. Ricci, *J. Am. Chem. Soc.* **2021**, *143*, 20296–20301.
[22] M. Pfeiffer, K. Trofymchuk, S. Ranallo, F. Ricci, F. Steiner, F. Cole, V. Glembockyte, P. Tinnefeld, *iScience* **2021**, *24*, 103072.
[23] E. Del Grosso, L. J. Prins, F. Ricci, *Angew. Chemie Int. Ed.* **2020**, *59*, 13238–13245.
[24] A. Amodio, E. Del Grosso, A. Troina, E. Placidi, F. Ricci, *Nano Lett.* **2018**, *18*, 2918–2923.
[25] S. W. Schaffter, L. N. Green, J. Schneider, H. K. K. Subramanian, R. Schulman, E. Franco, *Nucleic Acids Res.* **2018**, *46*, 5332–5343.
[26] D. Y. Zhang, G. Seelig, *Nat. Chem. 2011 32* **2011**, *3*, 103–113.
[27] H. Zhang, Y. Wang, H. Zhang, X. Liu, A. Lee, Q. Huang, F. Wang, J. Chao, H. Liu, J. Li, J. Shi, X. Zuo, L. Wang, L. Wang, X. Cao, C. Bustamante, Z. Tian, C. Fan, *Nat. Commun.* **2019**, *10*, DOI 10.1038/S41467-019-09004-4.
[28] M. Langecker, V. Arnaut, T. G. Martin, J. List, S. Renner, M. Mayer, H. Dietz, F. C. Simmel, *Science (80-.).* **2012**, *338*, 932–936.
[29] B. Saccà, R. Meyer, M. Erkelenz, K. Kiko, A. Arndt, H. Schroeder, K. S. Rabe, C. M. Niemeyer, B. Saccà, D.-C. R. Meyer, D.-B. M. Erkelenz, M. K. Sc Kiko, A. Arndt, H. Schroeder, K. S. Rabe, C. M. Niemeyer, *Angew. Chemie Int. Ed.* **2010**, *49*, 9378–9383.
[30] S. Ranallo, D. Sorrentino, F. Ricci, *Nat. Commun. 2019 101* **2019**, *10*, 1–9.
[31] L. N. Green, A. Amodio, H. K. K. Subramanian, F. Ricci, E. Franco, *Nano Lett.* **2017**, *17*, 7283–7288.
[32] A. Amodio, A. F. Adedeji, M. Castronovo, E. Franco, F. Ricci, *J. Am. Chem. Soc.* **2016**, *138*, 12735–12738.
[33] V. A. Turek, R. Chikkaraddy, S. Cormier, B. Stockham, T. Ding, U. F. Keyser, J. J. Baumberg, V. A. Turek, R. Chikkaraddy, S. Cormier, B. Stockham, T. Ding, U. F. Keyser, J. J. Baumberg, *Adv. Funct. Mater.* **2018**, *28*, 1706410.
[34] A. Kuzyk, Y. Yang, X. Duan, S. Stoll, A. O. Govorov, H. Sugiyama, M. Endo, N. Liu, *Nat. Commun. 2016 71* **2016**, *7*, 1–6.
[35] E. M. Willner, Y. Kamada, Y. Suzuki, T. Emura, K. Hidaka, H. Dietz, H. Sugiyama, M. Endo, *Angew. Chemie Int. Ed.* **2017**, *56*, 15324–15328.
[36] K. Jahnke, V. Huth, U. Mersdorf, N. Liu, K. Göpfrich, *ACS Nano* **2022**, *16*, 7233–7241.
[37] P. W. K. Rothemund, A. Ekani-Nkodo, N. Papadakis, A. Kumar, D. K. Fygenson, E. Winfree, *J. Am. Chem. Soc.* **2004**, *126*, 16344–16352.
[38] D. Y. Zhang, R. F. Hariadi, H. M. T. Choi, E. Winfree, *Nat. Commun. 2013 41* **2013**, *4*, 1–10.
[39] L. N. Green, H. K. K. Subramanian, V. Mardanlou, J. Kim, R. F. Hariadi, E. Franco, *Nat. Chem. 2019 116* **2019**, *11*, 510–520.
[40] N. Schormann, R. Ricciardi, D. Chattopadhyay, *Protein Sci.* **2014**, *23*, 1667–1685.
[41] S. Van Der Veen, C. M. Tang, *Nat. Rev. Microbiol. 2015 132* **2015**, *13*, 83–94.
[42] S. Boiteux, F. Coste, B. Castaing, *Free Radic. Biol. Med.* **2017**, *107*, 179–201.
[43] P. Handa, S. Roy, U. Varshney, *J. Biol. Chem.* **2001**, *276*, 17324–17331.
[44] S. S. Parikh, C. D. Putnam, J. A. Tainer, *Mutat. Res.* **2000**, *460*, 183–199.
[45] A. Biela, F. Coste, F. Culard, M. Guerin, S. Goffinont, K. Gasteiger, J. Ciešla, A. Winczura, Z. Kazimierczuk, D. Gasparutto, T. Carell, B. Tudek, B. Castaing, *Nucleic Acids Res.* **2014**, *42*, 10748.
[46] C. Rieux, S. Goffinont, F. Coste, Z. Tber, J. Cros, V. Roy, M. Guérin, V. Gaudon, S. Bourg, A. Biela, V. Aucagne, L. Agrofoglio, N. Garnier, B. Castaing, *Int. J. Mol. Sci.* **2020**, *21*, DOI 10.3390/IJMS21062058.
[47] J. M. Stewart, M. Viard, H. K. K. Subramanian, B. K. Roark, K. A. Afonin, E. Franco, *Nanoscale* **2016**, *8*, 17542–17550.
[48] A. R. Chandrasekaran, *Nanoscale* **2016**, *8*, 4436–4446.
[49] J. Mikkilä, A. P. Eskelinen, E. H. Niemelä, V. Linko, M. J. Frilander, P. Törmä, M. A. Kostiainen, *Nano Lett.* **2014**, *14*, 2196–2200.
[50] Y. X. Zhao, A. Shaw, X. Zeng, E. Benson, A. M. Nyström, B. Högberg, *ACS Nano* **2012**, *6*, 8684–8691.
[51] S. Sagredo, T. Pirzer, A. AghebatRafat, M. A. Goetzfried, G. Moncalian, F. C. Simmel, F. De La Cruz, *Angew. Chem. Int. Ed. Engl.* **2016**, *55*, 4348–4352.
[52] W. P. Klein, R. P. Thomsen, K. B. Turner, S. A. Walper, J. Vranish, J. Kjems, M. G. Ancona, I. L. Medintz, *ACS Nano* **2019**, *13*, 13677–13689.
[53] C. Sigl, E. M. Willner, W. Engelen, J. A. Kretzmann, K. Sachenbacher, A. Liedl, F. Kolbe, F. Wilsch, S. A. Aghvami, U. Protzer, M. F. Hagan, S. Fraden, H. Dietz, *Nat. Mater. 2021 209* **2021**, *20*, 1281–1289.
[54] Z. Zhang, Y. Yang, F. Pincet, M. C. Llaguno, C. Lin, *Nat. Chem.* **2017**, *9*, 653–659.

Entry for the Table of Contents

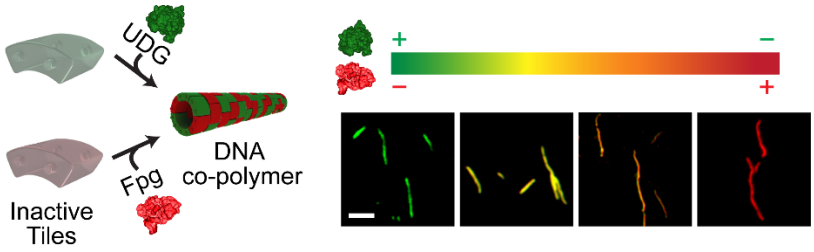

Table of Contents. We demonstrate here assembly of DNA co-polymers formed by two different tiles through the use of Base Excision Repair (BER) enzymes with highly predictable distribution.

Institute and/or researcher Twitter usernames: @RicciLab